Journal of Magnetism and Magnetic Materials 361 (2014) 249–254

Contents lists available at ScienceDirect

Journal of Magnetism and Magnetic Materials

journal homepage: www.elsevier.com/locate/jmmm

Use of triethylene glycol monobutyl ether in synthesis of iron oxide nanoparticles

Seda Beyaz [a], Fatmahan Ozel [b], Hakan Kockar [b,*], Taner Tanrisever [a]

[a] Department of Chemistry, Balikesir University, Balikesir 10145, Turkey
[b] Department of Physics, Balikesir University, Balıkesir 10145, Turkey

ARTICLE INFO

Article history:
Received 8 May 2013
Received in revised form
9 January 2014
Available online 21 February 2014

Keywords:
Magnetic material
Iron oxide
Nanostructure
Chemical synthesis

ABSTRACT

Superparamagnetic iron oxide nanoparticles were synthesized by thermal decomposition of iron–oleate complex using triethylene glycol monobutyl ether (TREGBE) as solvent for the first time for more mass of the nanoparticles. The effect of TREGBE on the properties of the nanoparticles was compared with that of 1-hexadecene. The impact of oleic acid concentration on the properties of the nanoparticles was also studied. On the use of TREGBE as compared with 1-hexadecene, the average crystal size reduced from 9.1 ± 2.1 to 8.2 ± 0.7 nm whereas the saturation magnetization (M_s) increased from 53.6 to 58.0 emu/g. Moreover, more products can be synthesized using TREGBE. Besides, the interactions between particle surfaces and TREGBE are weaker than that of 1-hexadecene according to gravimetric analysis results. X-ray diffraction analysis revealed that crystallinity and particle size scaled up with increasing oleic acid amount in TREGBE. The electron microscopy showed that dot-shaped particles turned into irregular particles with increasing amount of oleic acid molecules using TREGBE. The results disclosed that TREGBE is quite a suitable solvent to synthesize the superparamagnetic iron oxide nanoparticles with the desired size and M_s for more mass production at low temperature.

1. Introduction

Magnetic iron oxide nanoparticles (γFe_2O_3 and Fe_3O_4) have gained considerable attention in the past decade driven by their broad technological applications, including single-bit elements in high density magnetic data storage arrays [1], ferrofluids, magnetic refrigeration systems, photocatalysts, photoelectrodes, battery electrodes, magnetic inks for jet printing [2], contrast enhancement agents for magnetic resonance imaging [3], and magnetic carriers for drug targeting [4]. Among the synthesis methods of the iron oxide nanoparticles, thermal decomposition-based synthesis has proved a great success for the preparation of monodisperse nanoparticles [5–7]. This can also be done with high-temperature hydrolysis method [8,9]. This method is also suitable for mass production [10]. In thermal decomposition, many factors such as the nature of the precursor [11,12] and capping group [13], the concentration of precursor [14] and the decomposition temperature [10,15] affect the properties of the resulting particles. In some cases, a reducing or oxidizing agent may be required to obtain Fe(II) ion in the formation of magnetite. For instance, an alcohol is preferred in order to produce the partial reduction of the Fe^{3+} in case of iron (acetylacetonate) precursor [6]. In recent years, triethylene glycol molecules have been used for this purpose. In fact it has performed triple roles as a high-boiling solvent, reducing agent and stabilizer [16–18] which made this process easy to scale up for mass production. Generally, the polyol molecules are proposed for the preparation of easily reducible metals such as Pt, Ag, Au or Co [19]. However some metal oxide nanoparticles were also obtained by the polyol process [20] but the method is limited to polar precursors such as metal oxalate and metal acetates. The reducing agents are not required for iron–oleate complexes since a trace amount of CO, H_2, and carbon produced by the thermal decomposition of the complex is enough for the reduction of Fe^{3+} to Fe^{2+} [15]. But they can alter decomposition ratio of the complex and thus they can affect the product amount and particle size [10,15]. For instance, when the solvents with low boiling temperature such as hexadecene are used relatively poor decomposition occurs, resulting in less product and smaller particles [13].

This study presents a new solvent, triethylene glycol monobutyl ether (TREGBE; see Fig. 1), for mass production of iron oxide nanoparticles at low temperatures. The study investigated the properties of the resultant particles in TREGBE and compared them to those prepared in 1-hexadecene which has the same boiling

* Corresponding author. Tel.: +90 2666121278.
E-mail address: hkockar@balikesir.edu.tr (H. Kockar).

http://dx.doi.org/10.1016/j.jmmm.2014.02.032
0304-8853

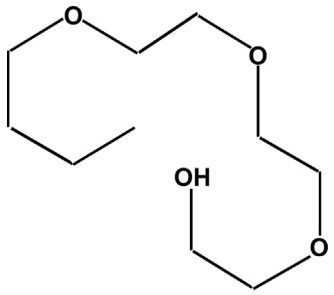

Fig. 1. Chemical structure of a TREGBE molecule.

point (280 °C). Besides, a series of nanoparticles were synthesized and characterized varying the concentration of oleic acid and the reaction time in the solvent of TREGBE. The results revealed that TREGBE provided higher magnetization and smaller particle size compared to 1-hexadecene probably due to its reducing character. Moreover, it is very suitable for mass production at low temperature, which provides efficient energy use for potential electronic and magnetic applications.

2. Experimental

The iron–oleate complex precursors were prepared using a published procedure [21]. In a typical experiment of this study, 2.7 g of $FeCl_3 \cdot 6H_2O$ (Merck, 99%) was dissolved in 50 mL of methanol (Merck, 99%) and then 3 equivalents oleic acid (Sigma-Aldrich, 99%) was added (9 mL) to the ferric salt. A solution with 1.2 g of NaOH (Merck, 99%) in 100 mL of methanol was dropped into this solution under magnetic stirring. The observed brown precipitate was washed with methanol 4–5 times and dried at 40 °C for 24 h.

By thermal decomposition of the iron–oleate complex, the magnetic iron oxide nanoparticles were synthesized in the different solvents with approximately the same boiling temperature: 1-hexadecene (Sigma-Aldrich, 92%) and TREGBE (Fluka, 70%). 0.9 g (1 mmol) of the iron–oleate complex and 10 mL of the chosen solvent were combined in a two-neck round-bottom reaction flask. The reaction mixture was then heated to about 274 °C using a temperature controller and with the temperature set at 300 °C it was refluxed for atleast 30 min. The initial reddish-brown color of the reaction solution turned brownish-black. The resultant solution was then cooled down to room temperature. In the use of 1-hexadecene solvent, a mixture of 10 mL of hexane (Merck, 95%) and 40 mL of acetone (Merck, 99%) was added to the reaction flask to precipitate the nanoparticles whereas the nanoparticles produced in TREGBE were precipitated by using water. All nanoparticles were separated under the magnet and washed 3 times by a mixture of hexane and acetone. After washing, they were collected using a magnet and dissolved in chloroform (Merck, 99%) to avoid aggregation in a liquid during storage time. All reaction conditions are listed in Table 1.

For the analysis of the Fourier transform infrared (IR) spectra, the samples dried by evaporating the chloroform were mixed with KBR powder and then recorded on a Perkin-Elmer spectrometer. X-ray diffraction (XRD) patterns were collected using a PANalytical's X'Pert PRO X-ray diffractometer system with a Cu-Kα source (1.54 Å). A high resolution transmission electron microscope (HRTEM, FEI TECNAI G^2 F30 model) with an accelerating voltage of 200 kV was used to obtain information of particle shape and size. Thermo-gravimetric analysis (TGA) was carried out using powder samples (~10 mg) with a heating rate of 10 °C/min using a Perkin-Elmer TG-DTA analyzer in air atmosphere up to 600 °C. Magnetic measurements were measured by a vibration sample magnetometer (VSM-ADE EV9 Model) at ±20 kOe. All measurements were carried out at room temperature.

Table 1
Synthesis conditions and results of the analysis.

Sample	Solvent type	Oleic acid (mL)	Reaction time (min)	HRTEM diameter (nm)	Crystallite size (nm)	M_s (emu/g)
H1	1-hexadecene	0	30	9.9 ± 2.0	9.1 ± 2.1	53.6
T1	TREGBE	0	30	8.6 ± 1.6	8.2 ± 0.7	58.0
T2	TREGBE	0.4	30	9.5 ± 1.7	8.5 ± 0.9	62.7
T3	TREGBE	0.9	30	9.2 ± 2.0	8.3 ± 0.8	68.2
T4	TREGBE	1.3	30	9.1 ± 2.2	8.4 ± 0.9	66.4
T5	TREGBE	2.2	30	11.4 ± 2.3	10.0 ± 0.2	31.6
T6	TREGBE	0.4	180	10.3 ± 1.6	9.0 ± 1.1	65.9

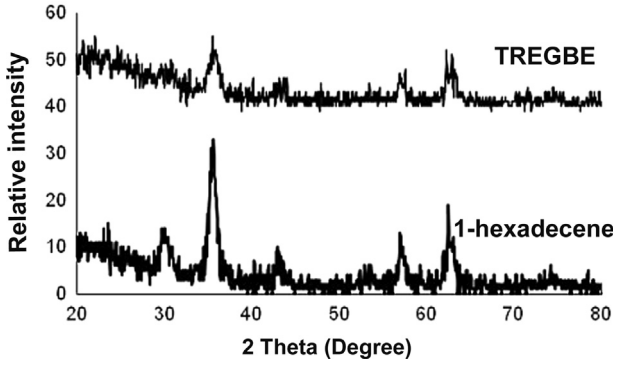

Fig. 2. XRD patterns of nanoparticles prepared in the 1-hexadecene solvent (sample H1) and TREGBE (sample T1).

3. Results and discussion

The properties of iron oxide nanoparticles prepared in the same experimental conditions but in different solvents, 1-hexadecene and TREGBE, were investigated comparatively. The effect of oleic acid amount on the properties of iron oxide nanoparticles prepared in TREGBE is discussed.

XRD patterns in Figs. 2–4 reveal a phase formation of magnetite or maghemite without contamination of other iron oxide phases. However, since their XRD patterns are very similar, it is difficult to distinguish the two phases simply from their XRD patterns.

The peak intensities in Fig. 2 indicate that the particles in 1-hexadecene have a higher crystallinity than the ones in TREGBE. This difference can be attributed to different mechanisms in the growth of crystals due to intervention of solvent molecules.

Fig. 3 presents a comparison of the XRD patterns of iron oxide nanoparticles prepared with various oleic acid concentrations. An increase was observed with addition of oleic acid in terms of crystallinity. Moreover, this trend is more pronounced at the highest oleic acid concentration (T5). Thus, it can be concluded that oleic acid causes the formation of more crystalline nanoparticles.

Average crystallite size of particles was calculated on the basis of the Scherrer equation [22] using the half maximum width of the intense peaks. For this, diffraction profile was fitted by a pseudo-Voight function [23] using the XFit program [24] and a line profile was obtained as shown in Fig. 4. The peaks used for size calculations were selected from those that have the best fit percentage. For example (220), (311), (511) and (440) peaks were used to calculate the average crystal size of T5 sample (see Fig. 4).

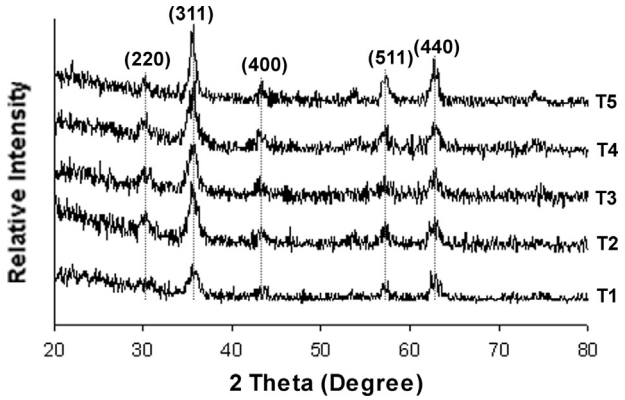

Fig. 3. XRD patterns of nanoparticles synthesized at various oleic acid concentrations (T1: no oleic acid, T2: 1 mmol, T3: 2 mmol, T4: 3 mmol, T5: 5 mmol oleic acid) with TREGBE.

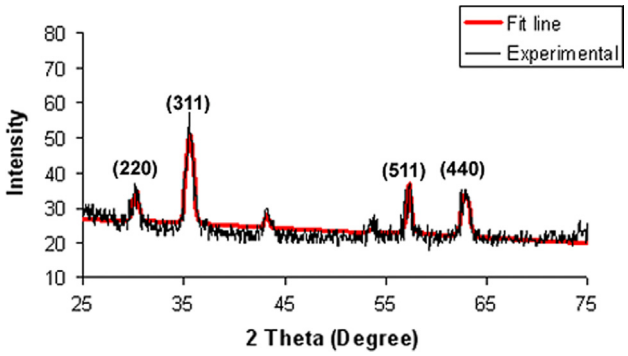

Fig. 4. XRD pattern and the fit profile line of synthesized T5 sample.

The HRTEM micrographs of the nanoparticles were also taken for comparison, and the particle sizes from the HRTEM and X-ray analysis, which are in good agreement, are summarized in Table 1. In comparison with the results of the methods, the average particle sizes from electron microscopy are larger than the crystal sizes estimated from X-ray analysis.

According to the XRD, the average crystal size was reduced when TREGBE was used as solvent instead of 1-hexadecene. As seen in the micrographs of sample H1 and sample T1 in Fig. 5, the decrease in particles size also was confirmed and the particles turned out to be dot-shaped in sample T1. Besides, narrower size distribution was observed for sample T1. It is also noticed that more product (0.32 g) can be synthesized using TREGBE when compared to the use of hexadecene (0.18 g). TREGBE was employed as a high-boiling solvent and reducing agent, as well as surfactant to prevent interparticle aggregation. This has allowed obtaining fine magnetic nanoparticles in shorter time.

It is disclosed that TREGBE increases decomposition of iron–oleate complexes since it is a reducing agent; thus a large number of nuclei are available in the nucleation stage. TREGBE is also a surfactant; thus the nucleus particles enlarge very little in the growth stage. Consequently, smaller particles are obtained in large quantities.

When the reaction time was increased in the TREGBE solvent, the particles enlarged and size distribution broadened as can be seen in Table 1 and Fig. 5. Electron microscopy images also revealed irregular angled particle shapes with increase in the reaction time. This trend which was reported many times for other solvents [12,15,21] is explained by the ripening process of the crystal particles in the solution [25].

Effect of surfactant concentration on particle size was examined by varying quantities of oleic acid and maintaining all other conditions in

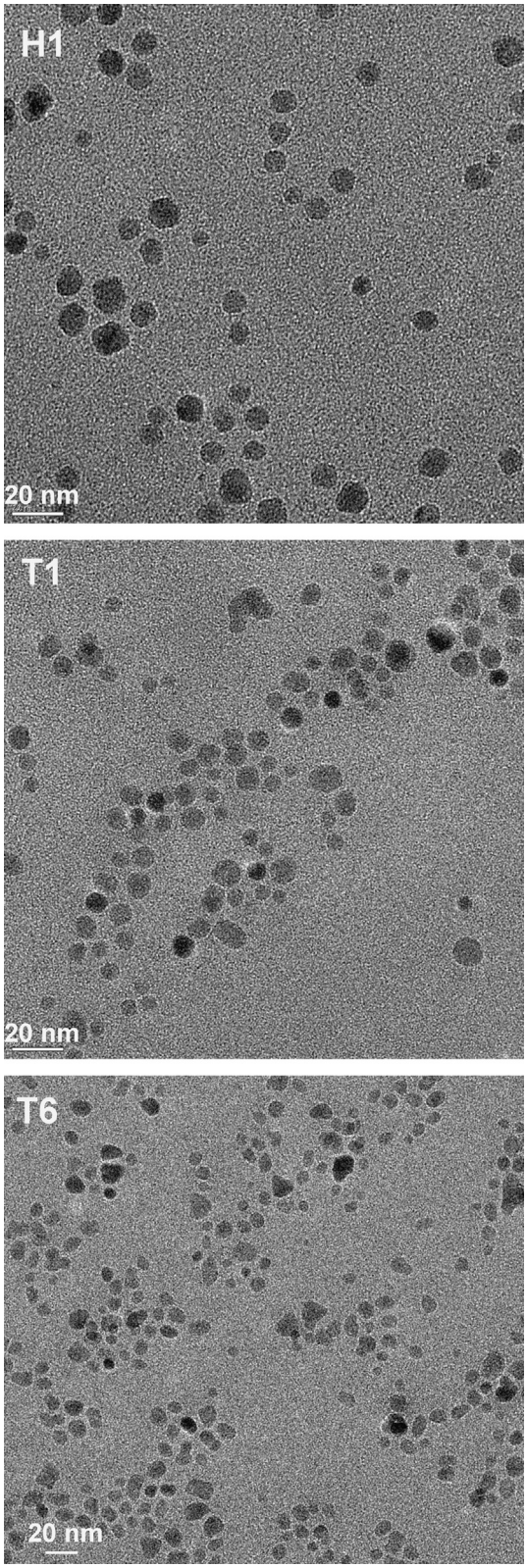

Fig. 5. HRTEM micrographs of iron oxides prepared in 1-hexadecene (sample H1) or in TREGBE (sample T1) at 30 min or in TREGBE at 180 min (sample T6).

TREGBE. The size results in Table 1 and Fig. 6 showed that the particle size remained unchanged for a range of 1–3 mmol of oleic acid, but then increased remarkably with addition of 5 mmol oleic acid. The studies [11,13,26] show that oleic acid works as a mild catalyst and provides an effective steric barrier during the reaction. However, its

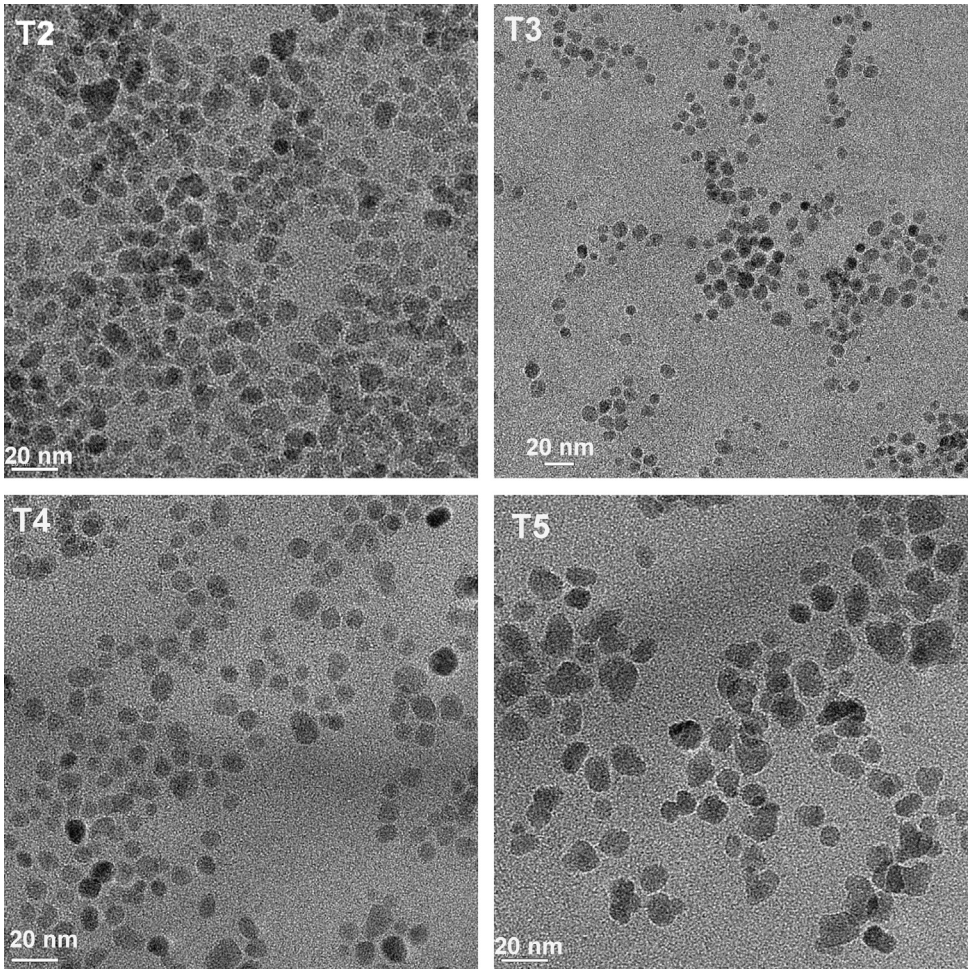

Fig. 6. HRTEM images of iron oxide nanoparticles prepared with various oleic acid amounts (mmol) samples T2: 1, T3: 2, T4: 3, and T5: 5.

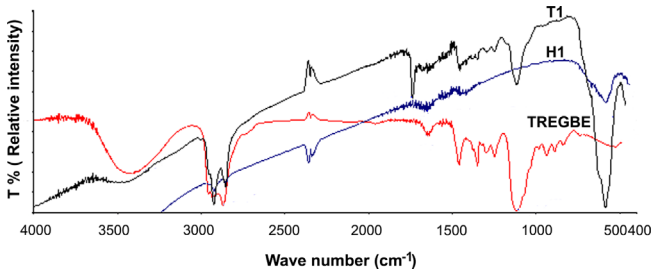

Fig. 7. IR spectrums of pure TREGBE and nanoparticles (sample T1 and H1) prepared without oleic acid in TREGBE.

molecules form a complex with iron species giving rise to intermediate complexes and this causes a delay in the nucleation, which results in more particles with larger sizes [13]. For example, 11 nm, 12 nm and 14 nm iron oxide nanocrystals were synthesized using solutions with oleic acid concentrations of 1.5 mM, 3 mM and 4.5 mM, respectively, by Park et al. [10]. Hyeon et al. [5] and Yin et al. [13] declared that when the molar ratio of $Fe(CO)_5$ to oleic acid was higher than 1:5, nanocrystals did not form due to hindered nucleation. Thus, it can be said that the trend of increasing size with increasing amount of oleic acid was not observed up to 4 mmol owing to probably the TREGBE molecules which accelerate the nucleation and hinder the formation of the complex giving an esterification reaction with carboxyl head of oleic acid (see Fig. 7). As oleic acid concentration was increased, particle size distribution was broadened according to electron microscopy results in Table 1. Besides, HRTEM micrographs in Fig. 6 also indicated that the shapes of nanoparticles were not uniform. In particular, iron oxide nanoparticles (T5) prepared with the highest oleic acid amount have highly irregular shapes. It seems that excess amount of oleic acid gives rise to a small nucleus but longer growth of crystal and thus there are rearrangements on the crystal surface for favorable energetic faces such as {111}, {110}, or {100} [27].

Fig. 7 presents the IR spectrum of iron oxide nanoparticles prepared without oleic acid in the different solvents, as well as pure TREGBE solvent. It is obvious that the characteristic band of the TREGBE at 1116 cm^{-1}(–R–O–R) is present in iron oxide nanoparticles, indicating the binding of TREGBE to iron oxide nanoparticles [28]. However, the strength and sharpness of characteristic free OH band at 3423 cm^{-1} in spectrum of TREGBE reduced whereas a new band at 1734 cm^{-1} appeared in the spectrum of the nanoparticles. The reason is that a carboxylic acid group combined with alcohol group of the TREGBE molecule by a typical esterification reaction and hence the long surfactants including an ester group formed on the surface of nanoparticles. Besides, while asymmetric vibration [29] between the carboxylate head and the metal atom was observed only at 1454 cm^{-1}, a very broad band was seen in the symmetric vibration region of carboxylates (1650–1510) because of overlapping with O–H bending [30] at 1643 cm^{-1} attributed for water and the TREGBE molecules adsorbed to the particle surface [16–18].

To better understand the interactions of capping agents on surface of the particle, thermal gravimetric analysis of sample H1 and sample T1 was carried out and is presented in Fig. 8. Two distinct weight losses for both samples between room temperature

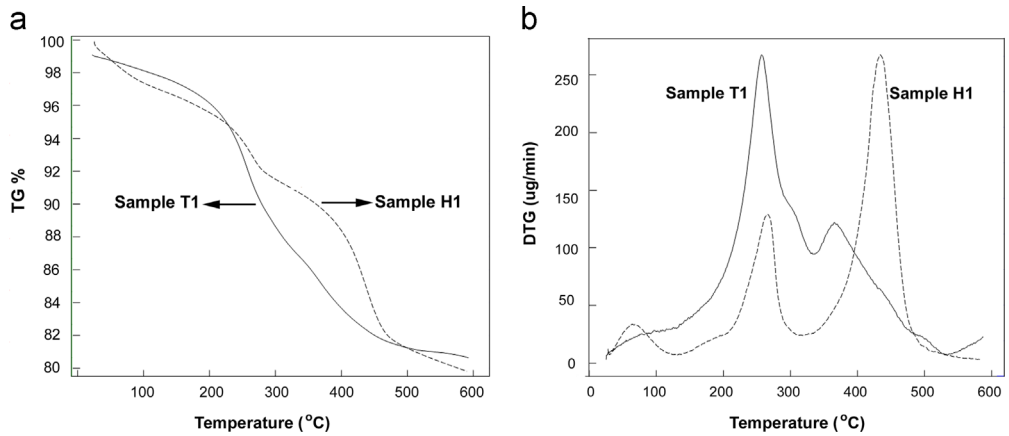

Fig. 8. TGA–DTA results of iron oxide nanoparticles prepared in different solvents without surfactant: percentages (a) and derivatives (b) of weight losses.

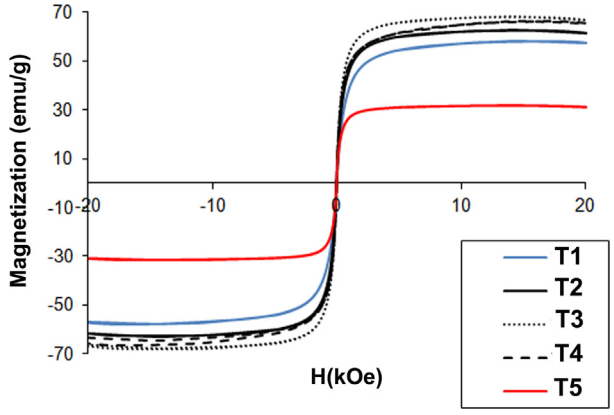

Fig. 9. The magnetization curves of iron oxide nanoparticles prepared in TREGBE varying the amount of oleic acid: (T1: 0, T2: 1 mmol, T3: 2 mmol, T4: 3 mmol, and T5: 5 mmol).

and 600 °C can be seen in Fig. 8(b). However, the first weight loss (10.0%) of sample T1 is higher than that (5.6%) of sample H1, but the second weight loss (5.6%) is lower than that (10.4%) of H1. Moreover, the second transition temperature (370 °C) of the sample T1 with TREGBE is lower than that (420 °C) of sample H1 too. Consequently, it can be said clearly that the interaction between particle surface and TREGBE is weaker than that of 1-hexadecene. Additionally, for sample T1, the first step which represents the most significant weight loss could be attributed to the removal of residual TREGBE in the sample whose boiling point is around 280 °C. Thus, it is also seen that the presence of TREGBE on the surface of the iron oxide nanoparticles is supported by the TGA measurement.

Magnetization curves of the nanoparticles illustrated at ± 20 kOe are shown in Fig. 9 since they reached the saturation values. As the magnetic field intensity reversed, the magnetization decreased from the plateau value and reached about zero. The saturation magnetizations are listed in Table 1. It is revealed that the magnetite nanoparticles have superparamagnetic properties with zero coercivity, H_c.

In comparison with solvents, the M_s value of sample T1 prepared in TREGBE was found to be higher than H1 sample's in 1-hexadecene whereas the H_c value of T1 sample is lower than that of sample H1 as seen in Table 1. As clearly explained in the TGA analysis, the weaker interactions on nanoparticles with TREGBE can allow magnetic arrangement easily, which leads to higher magnetization. Thus it can be concluded that TREGBE has better magnetic properties than that of 1-hexadecene.

When the amount of oleic acid was increased gradually, the M_s increased up to 68 emu/g and then decreased to 32 emu/g (see Fig. 9 and Table 1). It is already known that oleic acid molecules are bonded to the Fe(II) or Fe(III) on the particle surface through carboxyl group that has a strong influence on its magnetic behavior, particularly a positive effect on the saturation magnetization [31,32]. This effect can be observed at low oleic acid concentrations; however, the magnetic moment per gram measured by the VSM diminishes since the number of nonmagnetic long surfactants (see the IR spectrum) on the particle surface increases with more addition of oleic acid. Thus, the effect of high oleic acid amount on the magnetization was masked by nonmagnetic long surfactants caused by esterification between TREGBE and oleic acid.

As the reaction time increased, M_s value slightly increased from 62.5 emu/g to 65.9 emu/g (see Table 1). This result can be attributed to the increase of particle size [6] (Fig. 5).

4. Conclusions

In this study, the first time use of TREGBE as a solvent was performed to synthesize superparamagnetic iron oxide nanoparticles by thermal decomposition method. It was observed that usage of TREBGE led to obtaining 15% smaller particles and 8% higher magnetization in comparison with those prepared in 1-hexadecene. Furthermore, the product amount also increased up to 78% with the use of TREGBE. Thus, the TREBGE procedure was found to be more useful for mass production of nanoparticles and also an easier way than the one obtained with current possible methods. These advantages can be attributed to be high nucleus number as a result of increase of the decomposition rate by TREGBE.

Acknowledgments

This work is supported by TUBITAK, Turkey, under Grant no. 109T017 and also partly by Balikesir University, Turkey (BAP 2008/04). The authors would like to thank State Planning Organization, Turkey, under Grant no. 2005K120170 for the VSM system and Bilkent University, UNAM, for HRTEM analysis. Thanks also go to H. Guler, Balikesir University, for XRD measurements.

References

[1] M. Muhammed, T. Tsakalakos, J. Korean Ceram. Soc. 11 (2003) 1027.
[2] A. Lu, E.L. Salabas, F. Schutch, Angew. Chem. Int. Ed. 46 (2007) 1222.
[3] S. Laurent, D. Forge, M. Port, A. Roch, C. Robic, L.V. Elst, R.N. Muller, Chem. Rev. 108 (2008) 2064.
[4] M. De, P.S. Ghosh, V.M. Rotello, Adv. Mater. 20 (2008) 4225.
[5] T. Hyeon, S. Lee, J. Park, Y. Chung, H.B. Na, J. Am. Chem. Soc. 123 (2001) 12798.
[6] S. Sun, H. Zeng, J. Am. Chem. Soc. 124 (28) (2002) 8204.
[7] W.W. Yu, J.C. Falkner, C.T. Yavuz, V.L. Colvin, Chem. Commun. 20 (2004) 2306.

[8] H. Xia, L. Zhang, Q. Chen, L. Guo, H. Fang, X. Li, J. Song, X. Huang, H. Sun, Phys. Chem. C 113 (2009) 18542.
[9] J. Ge, Y. Hu, M. Biasini, W.P. Beyermann, Y. Yin, Angew. Chem. Int. Ed. 46 (2007) 4342.
[10] J. Park, K. An, Y. Hwang, J.G. Park, H.J. Noh, J.Y. Kim, J.H. Park, N.M. Hwang, T. Hyeon, Nat. Mater. 3 (12) (2004) 891.
[11] A.G. Roca, M.P. Morales, C.J. Serna, IEEE Trans. Magn. 42 (10) (2006) 3025.
[12] F.X. Redl, C.T. Black, G.C. Papaefthymiou, R.L. Sandstrom, M. Yin, H. Zeng, C.B. Murray, S.P. O'Brien, J. Am. Chem. Soc. 126 (2004) 14583.
[13] M. Yin, A. Willis, F. Redl, N.J. Turro, S.P. O'Brein, J. Mater. Res. 19 (4) (2004) 1208.
[14] S. Chaianansutcharit, O. Mekasuwandumrong, P. Praserthdam, Cryst. Growth Des. 6 (2006) 141.
[15] S.G. Kwon, Y. Piao, J. Park, S. Angappane, Y. Jo, N. Hwang, J. Park, T. Hyeon, J. Am. Chem. Soc. 129 (2007) 12571.
[16] D. Maity, S.N. Kale, R.K. Ghanekar, J.-M. Xue, J. Ding, J. Magn. Magn. Mater. 321 (2009) 3093.
[17] J. Wan, W. Cai, X. Meng, E. Liu, Chem. Commun. 47 (2007) 5004.
[18] W. Cai, J. Wan, J. Colloid Interface Sci. 305 (2007) 366.
[19] C. Liu, X. Wu, T. Klemmer, N. Shukla, X. Yang, D. Weller, A.G. Roy, M. Tanase, D. Laughlin, J. Phys. Chem. B 108 (20) (2004) 6121.
[20] C. Feldmann, Scr. Mater. 44 (2001) 2193.
[21] N.R. Jana, Y. Chen, X. Peng, Chem. Mater. 16 (20) (2004) 3931.
[22] M. Abdullah, M. Khairurrijal, J. Nano Saintek 1 (2008) 28.
[23] F. Sanchez-Bajo, L. Cumbrera, J. Appl. Crystallogr. 30 (1997) 427.
[24] R.W. Cheary, A.A. Coelho, Software: Xfit-Koalariet CCP14 Library, ⟨http://www.ccp14.ac.uk⟩, 1996.
[25] J. Park, J. Joo, S.G. Kwon, Y. Jang, T. Hyeon, Angew. Chem. Int. Ed. 46 (2007) 4630.
[26] L. Zhang, R. He, H. Gu, Appl. Surf. Sci. 253 (2006) 2611.
[27] J. Cheon, X. Kang, S.-M. Lee, J.-H. Lee, J.-H. Yoon, S.J. Oh, J. Am. Chem. Soc. 126 (2004) 1950.
[28] J.R. Dyer, Applications of Absorption Spectroscopy of Organic Compounds, Prentice-Hall, Inc., Englewood Cliffs, NJ, 1965.
[29] L.M. Bronstein, X. Huang, J. Retrum, A. Schmucker, M. Pink, B.D. Stein, B. Dragnea, Chem. Mater. 19 (2007) 3624.
[30] J.J. Max, C. Chapados, J. Chem. Phys. 131 (2009) 184505.
[31] A.G. Roca, M.P. Morales, K. O'Grady, C.J. Serna, Nanotechnology 17 (2006) 2783.
[32] C. Yu, W. Jian, M. Hong, G. Chen, Y. Zhang, N. Gu, Chin. Chem. Lett. 21 (2010) 179.